Current Optics and Photonics
Vol. 4, No. 2, April 2020, pp. 115-120

ISSN: 2508-7266(Print) / ISSN: 2508-7274(Online)
DOI: https://doi.org/10.3807/COPP.2020.4.2.115

Analytical Study of the Image Reconstruction of Fourier Holograms Using Varifocal Electric-Field-Driven Liquid Crystal Fresnel Lenses

Taehyeon Kim, Seung-Chul Lee, and Woo-Sang Park*

Department of Electronic Engineering, Inha University, Incheon 22212, Korea

(Received November 5, 2019 : revised January 3, 2020 : accepted January 17, 2020)

A novel method is proposed for controlling the distance of an image plane in Fourier holograms using varifocal electric-field-driven liquid-crystal (ELC) lenses. Phase Fresnel lenses are employed to reduce the thickness and response time of the ELC lenses. The voltages applied to the electrodes of the ELC Fresnel lens are adjusted so that the lens has the same retardation distribution as an ideal lens. The focal length can be controlled by changing the retardation distribution with the applied voltages. Simulations were conducted for the image reconstruction of Fourier holograms with various focal lengths of the ELC Fresnel lenses. The simulation results indicate that the distance of the image plane can be properly controlled with the varifocal ELC Fresnel lens.

Keywords : Computer generated hologram, 3D image reconstruction, Liquid-crystal lens
OCIS codes : (090.1760) Computer holography; (230.3720) Liquid-crystal devices; (090.1995) Digital holography

I. INTRODUCTION

Fourier, Fresnel, and image holograms are well-known types of holograms [1-3]. A Fourier hologram is a recording of waves with the object field on the front focal plane of the lens and the holographic recording medium on the back focal plane. For reconstruction, the image is formed on the back focal plane of the lens by placing a hologram fringe on the front focal plane and illuminating reference waves [1]. A Fourier hologram uses the Fourier transforming properties of the lens, so it is relatively easy to calculate computer-generated holograms (CGHs) in digital holograms, and the noise can be reduced relatively easily through a mask and a filter as the waves are divided into DC component, conjugate, and primary images on the image plane. As a Fourier hologram requires the use of lenses, however, the system configuration is complicated, the image quality is affected by lens aberration, and the viewing zone is fixed to the focal plane of the lens.

We propose a hologram scheme to simplify the system configuration and to control the focal plane by integrating liquid crystal spatial light modulators (LC-SLMs) and electric-field-driven liquid crystal (ELC) lenses as imaging lenses in Fourier hologram reconstruction. The ELC lens can function as a converging lens as the retardation caused by the applied voltage in each electrode changes the wavefront of the optic waves into spherical waves [4]. A varifocal lens can be realized by adjusting the voltage applied to each electrode to determine the retardation according to the focal length of the lens. The ELC lens was designed in the form of a Fresnel lens to reduce the thickness of the liquid crystal layer, which enables a fast response time. The system was validated by calculating a reconstructed image on the image plane according to each focal length using the Huygens-Fresnel principle. The quality of the reconstructed image was quantitatively evaluated by comparing the relationship between the root-mean-square (RMS) value and peak signal-to-noise (PSNR) of the image according to the focal length of the varifocal ELC Fresnel lens.

*Corresponding author: wspark@inha.ac.kr, ORCID 0000-0001-6087-5595
Color versions of one or more of the figures in this paper are available online.

II. PROPOSED METHOD

2.1. Fourier Holograms with Varifocal ELC Lens

Figure 1 shows a diagram of the proposed varifocal Fourier hologram system. In the hologram configuration, the LC-SLM is assembled to the varifocal ELC lens on the plane by moving the hologram plane from the original location of the plane to the plane at distance equal to the focal length *f*. Therefore, the interference pattern appearing on the LC-SLM should have the form in which CGH on the plane is propagated by the focal length of the ELC lens. The ELC lens is designed to have the same size as the LC-SLM.

Figure 2 shows the structure of the varifocal ELC Fresnel phase lens used in the hologram system. The liquid crystal molecules of the ELC lens are homogeneously aligned parallel to the polarizer direction of the SLM so that maximum retardation occurs in the field-off state. The retardation distribution for each electrode was optimized by designing the common electrode as well as the driving electrode to have a multiple-electrode structure [5]. As the electrode width and the interelectrode spacing become shorter, the lens retardation distribution can be finely and accurately adjusted. However, the tangential component of the electric field between neighboring electrodes can cause distortion of the liquid crystalline behavior, so the width and the spacing of the electrode were designed by considering the process conditions as 20 and 4 μm, respectively. The retardation at each position of the lens was obtained by calculating the behavior of the liquid crystal molecules caused by the voltage applied to the electrodes through a 3-dimensional numerical method using de Gennes' order tensor and the Erickson-Leslie equation of motion [6]. The birefringence Δn of the liquid crystal used in the calculation is 0.1928, and the thickness d of the liquid crystal layer of the ELC lens is 35 μm.

Figure 3 shows the retardation of the liquid crystal layer caused by the applied voltage. As the voltage applied to the electrode increases, the liquid crystal molecules with positive dielectric anisotropy will tend to align close to perpendicular to the glass surfaces. As a result, the retardation decreases when the polarized light from the

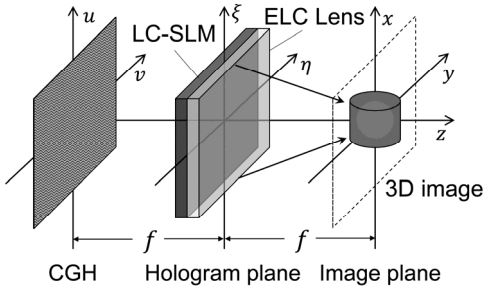

FIG. 1. Diagram of the varifocal Fourier holograms with ELC lens.

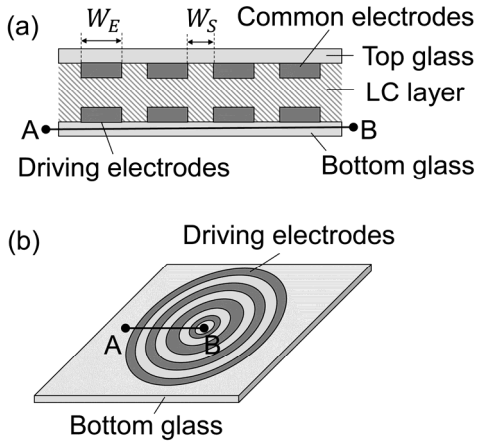

FIG. 2. Diagram of the ELC Fresnel lens: (a) cross-sectional view and (b) top view of the bottom glass. W_E and W_S are the width of the electrode and interelectrode spacing, respectively.

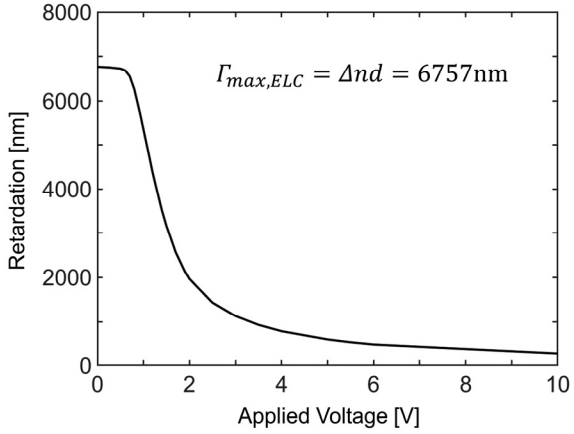

FIG. 3. Retardation of the ELC lens according to the applied voltage. $\Gamma_{\text{max,ELC}}$ is the maximum retardation of the ELC lens with birefringence Δn = 0.1928 and thickness d = 35 μm. The ELC lens exhibits the maximum retardation in the off state.

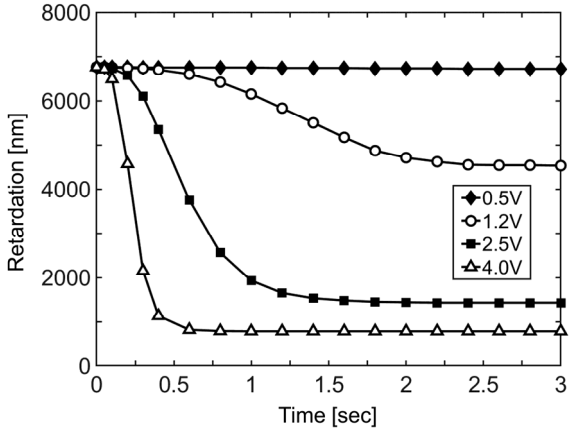

FIG. 4. Retardation over time after applying voltages to the liquid-crystal layer in the ELC lens.

SLM is transmitted through the liquid crystal layer. The retardation distribution required for each driving electrode of the ELC lens with a specific focal length must coincide with the retardation distribution of an ideal Fresnel phase lens. To achieve this, the relationship between the voltage and the retardation in Fig. 3 is used to determine the voltage applied to each driving electrode of the ELC lens.

Figure 4 shows the retardation over time according to the voltage applied to the driving electrode of the ELC lens. The response time of the liquid crystal in the ELC lens is determined by the elapsed time until the retardation indicates a constant value after a voltage is applied. A lower voltage results in weaker electric field intensity applied to the liquid crystal molecules, so the response time decreases. Therefore, the liquid crystal on the driving electrode, which requires large retardation for a short focal length, shows a relatively slow response time.

Figures 5(a) and 5(b) show the retardation distribution of the ideal Fresnel lens for different focal lengths, and Figs. 5(c) and 5(d) show the results for the ELC Fresnel lens. The number of grooves in the ELC Fresnel lens with the same groove depth is determined by the maximum retardation $\Gamma_{\mathrm{max,ideal}}$ for obtaining the focal length of an ideal single convex lens and the maximum retardation of the liquid crystal layer $\Gamma_{\mathrm{max,ELC}}$ as follows:

$$\text{number of grooves} = ceil(\Gamma_{\mathrm{max,ideal}} / \Gamma_{\mathrm{max,ELC}}). \quad (1)$$

In this equation, $ceil(x)$ is a ceiling function, and $\Gamma_{\mathrm{max,ideal}}$ is the maximum optical path difference of the convex lens. The maximum retardation of the ELC lens $\Gamma_{\mathrm{max,ELC}}$ is determined by the refractive index birefringence of the liquid crystal when no voltage is applied. As the focal length decreases, as shown in Fig. 5, the retardation of the lens increases, and the number of grooves increases accordingly.

For the retardation distribution of the ELC Fresnel lens of Figs. 5(c) and 5(d), a quantized retardation distribution is observed when comparing the result with the ideal case in Figs. 5(a) and 5(b). This occurs because of the driving electrode of the ELC lens with a certain size. In particular, rapid variation of the retardation cannot be realized at the position where the retardation of the Fresnel lens is discontinuous. This leads to a section with a large difference from the values of the ideal case in Figs. 5(a) and 5(b). In addition, an increase in the number of grooves due to the short focal length in the ELC lens results in a degradation of the reconstructed image by intensifying the mismatch against the ideal retardation distribution.

Figure 6 shows the RMS value of the two-dimensional wavefront error. The retardation distribution difference between the ideal Fresnel lens and ELC Fresnel lens was evaluated quantitatively by the focal length. The wavelength used in the evaluation is 632 nm. A shorter focal length of the ELC lens results in higher RMS error, which causes noise in the image during hologram reconstruction.

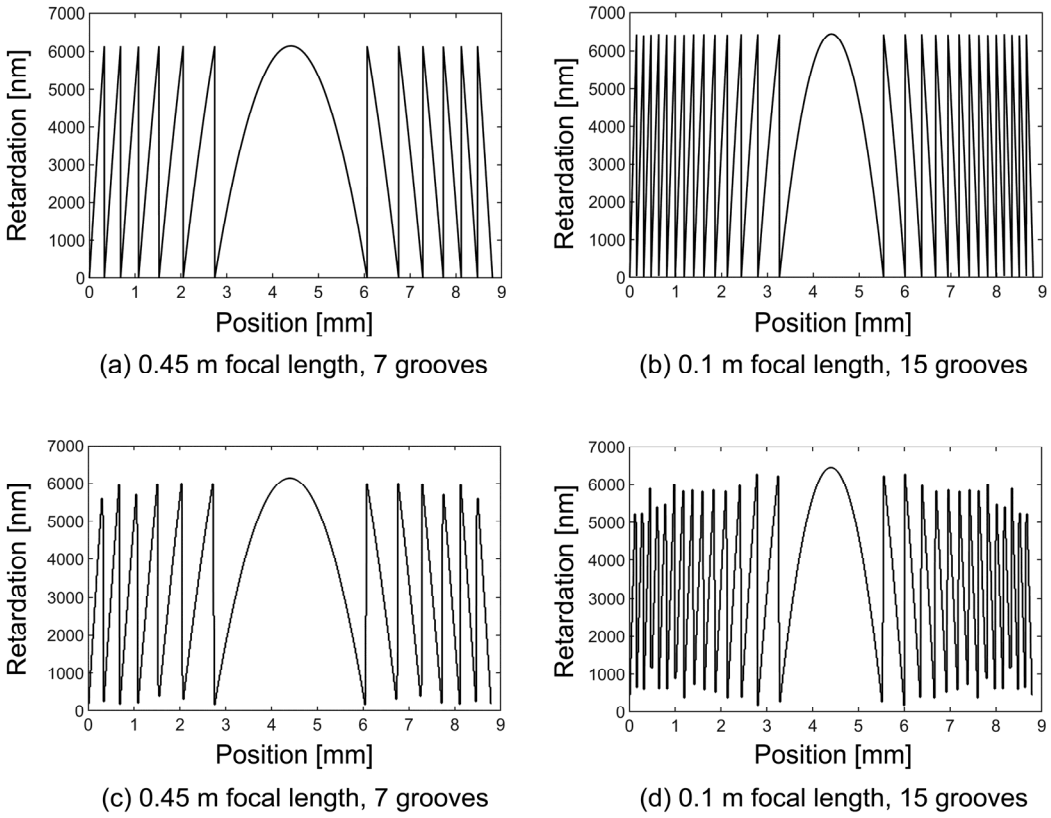

FIG. 5. Distributions of the retardation in (a, b) ideal Fresnel lenses and (c, d) the ELC lenses.

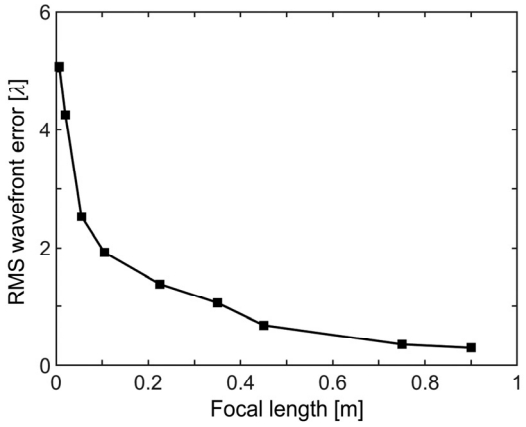

FIG. 6. RMS wavefront error according to focal length of the ELC lens. λ is the number of wavelengths based on the wavelength of 632 nm.

2.2. Theoretical Calculation of Hologram Reconstruction

The image plane in a Fourier hologram is formed on the back focal plane of the lens, and the reconstructed image on the image plane is represented by the Fourier transform of the interference fringes on the SLM. Because the proposed ELC lens is not an ideal converging lens and the system is configured so that the SLM and ELC lens are in the same plane, however, the field propagated to the back focal plane cannot be calculated by Fourier transform. Therefore, in this simulation, the field $U(x,y)$ in the image plane is calculated from the following equation using the Fresnel diffraction integral derived from the Huygens-Fresnel principle [7]:

$$U(x,y)=\frac{e^{jkf}}{j\lambda f}\exp\left(j\frac{k}{2f}(x^2+y^2)\right) \cdot \iint\left\{U(\xi,\eta)\exp\left(j\frac{k}{2f}(\xi^2+\eta^2)\right)\right\}e^{-j\frac{k}{f}(x\xi+y\eta)}d\xi d\eta . \tag{2}$$

In this equation, $\exp\left(j\frac{k}{2f}(x^2+y^2)\right)$ denotes the point-spread function in free space, and $U(\xi,\eta)$ is the intensity of the field after passing through the lens, which can be expressed as follows:

$$U(\xi,\eta)=s'(\xi,\eta)t(\xi,\eta) . \tag{3}$$

In Eq. (3), $t(\xi,\eta)$ is a transfer function that is determined by the retardation data of the ELC lens. $s'(\xi,\eta)$ is the interference pattern appearing on the SLM. In a conventional Fourier hologram, the SLM is located in the front focal plane of the lens, so the interference pattern $s(u,v)$ is equal to the inverse Fourier transform of the image to be reconstructed in the back focal plane. However, because the SLM in our hologram system is on the same plane as the ELC lens, the field $s'(\xi,\eta)$ propagated by the focal length instead of $s(u,v)$ becomes the interference pattern of the SLM, as shown in the following equation:

$$s'(\xi,\eta)=\frac{e^{jkf}}{j\lambda f}\exp\left(j\frac{k}{2f}(\xi^2+\eta^2)\right) \cdot \iint\left\{s(u,v)\exp\left(j\frac{k}{2f}(u^2+v^2)\right)\right\}e^{-j\frac{k}{f}(\xi u+\eta v)}dudv . \tag{4}$$

In other words, the image reconstruction by the hologram can be obtained by calculating the intensity on the image plane using the Fresnel diffraction integral of the SLM interference pattern and transfer function of the ELC lens. The resolution of the SLM used in the calculation is 1920 × 1080, and the pixel pitch is 4 μm. The wavelength of the hologram reference beam is 632.9 nm. Since the size of the ELC lens is the same as that of the SLM, and the diagonal length of the SLM, the electrode width and the interelectrode distance of the ELC lens are 0.881 cm, 20 μm, and 4 μm, respectively, the number of electrodes of the ELC lens is 184 in total.

III. SIMULATION RESULTS AND DISCUSSION

Figure 7 shows the object image and the simulation results of the reconstructed image using the ideal lens and the ELC lens. Figure 7(a) shows the object image obtained from the point cloud composed of the spatial distance information for each point of an object on the hologram plane basis [8]. The object image is converted to CGH data and used to obtain the SLM interference fringes. Figure 7(b) shows the calculation results obtained using an ideal lens, and Figs. 7(c)~7(f) show the results of reconstructing the interference pattern of the SLM at the corresponding focal length according to the focal length of the ELC Fresnel lens. In the calculation, the focal lengths were taken as 0.07 m, 0.1 m, 0.3 m, and 0.45 m, as typical values, in the range of 0.07 to 0.45 m of focal length, where the RMS wavefront error of the ELC lens changes significantly as shown in Fig. 6. As can be seen in the figures, the result of the ELC lens is reconstructed with a similar shape to that of the ideal lens, but some results show that the aberration causes a noise distribution of the fringe pattern on the object surface. Figures 7(c)~7(f) indicate that the noise increases as the focal length of the ELC lens decreases. In particular, Fig. 7(c) shows that because the RMS wavefront error of the ELC lens is as large as 2.5 wavelengths, the wavefront of the light passing through the lens does not form a perfect sphere and the wave does not converge to the image plane, thereby preventing the image from being clearly reproduced. In order to obtain fairly good quality of the reconstructed images using the ELC lens, it is necessary to have a focal length of 0.3 m or more corresponding to

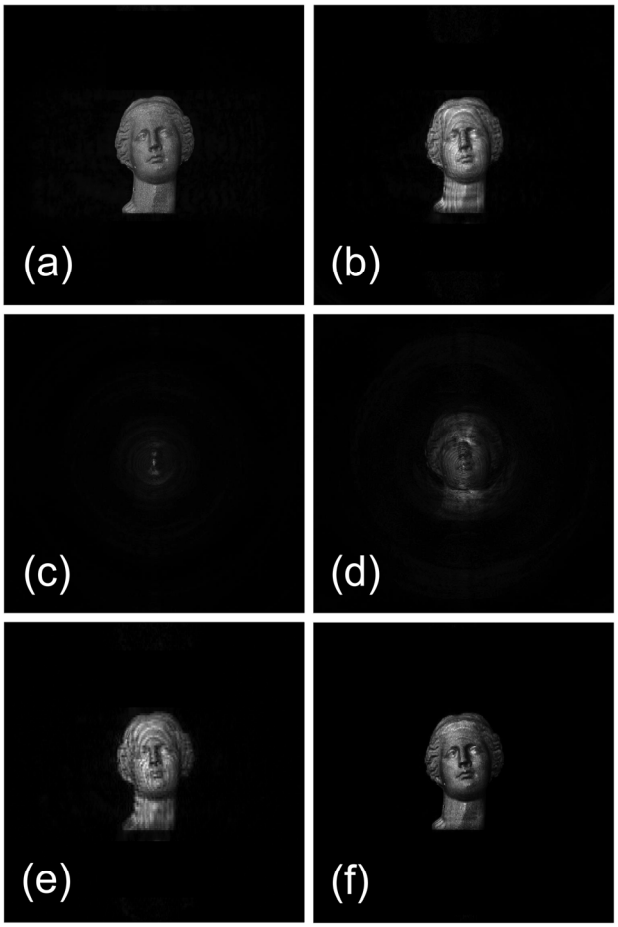

FIG. 7. (a) Object image calculated using the wave amplitude and phase information for the object surface obtained from the mesh data in the point cloud. Numerical reconstruction by Fourier hologram using (b) an ideal lens with focal length of 0.3 m and the ELC Fresnel lens with focal lengths of (c) 0.07 m, (d) 0.1 m, (e) 0.3 m, and (f) 0.45 m.

RMS wavefront error of at least one wavelength, as shown in the figures.

Figure 8 shows the PSNR of the reconstructed images of the hologram for the quantitative evaluation of noise. In the calculation of PSNR, the reference image is set to the image reproduced by an ideal lens with the same focal length, and the peak value is set to 255, which is the maximum value of an 8-bit grayscale image. As the focal length of the ELC lens decreases, PSNR of the reconstructed image decreases and the noise component that does not converge at the focal length increases. The decrease in PSNR arises from the increase in waves that do not converge on the focal plane among the waves incident on the ELC lens. This occurs because the discrepancy between the quantized retardation of the ELC lens and the retardation of the ideal lens increases as the focal length of the ELC lens decreases. These results are consistent with the results of noise phenomena according to the focal length of the ELC lens using the RMS wavefront error in Fig. 6.

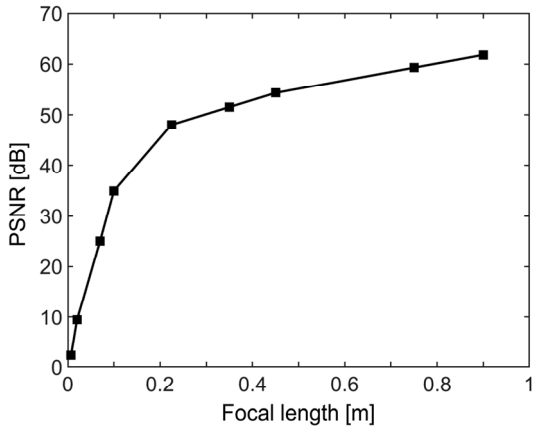

FIG. 8. PSNR of the reconstructed image according to the focal length of the ELC lens.

IV. CONCLUSION

A method has been proposed to control the hologram reconstruction distance with a varifocal ELC Fresnel lens for Fourier hologram image reconstruction. The varifocal ELC lens was made in the form of a Fresnel lens to reduce the thickness and response time. The retardation of the lens was obtained by calculating the behavior of the liquid crystal molecules according to the voltage applied to the electrode of the lens. The focal length of the ELC lens was controlled by appropriately adjusting the voltage applied to each electrode of the lens so that the retardation distribution of the ELC lens was the same as that of an ideal lens. The RMS wavefront error was calculated to quantitatively evaluate the quality of the ELC lens.

The simulation results showed that as the focal length increases, the RMS value decreases and the ELC lens becomes more similar to an ideal lens. The reconstructed image on the image plane of the Fourier hologram with the ELC lens was verified by using the Fresnel diffraction integral to simulate light waves passing through an SLM diffraction pattern and ELC lens. By using the ELC Fresnel lens in the simulation, it was possible to vary the reconstruction position of the reconstructed image of the hologram and obtain 3-D images of fairly good quality. In addition, as the focal length decreased, the RMS wavefront error of the waves passing through the lens increased, which led to degradation of the reconstructed image quality of the hologram. The calculation results showed that reconstructing hologram images of sufficiently good quality requires an ELC lens with a focal length of 0.3 m or more, which corresponds to an RMS wavefront error of one wavelength or less.

ACKNOWLEDGMENT

This study was supported by Inha University research grant.

REFERENCES

1. Y. Li, D. Abookasis, and J. Rosen, "Computer-generated holograms of three-dimensional realistic objects recorded without wave interference," Appl. Opt. **40**, 2864-2870 (2001).
2. D. Abookasis and J. Rosen, "Three types of computer-generated hologram synthesized from multiple angular viewpoints of a three-dimensional scene," Appl. Opt. **45**, 6533-6538 (2006).
3. Y. Sando, M. Itoh, and T. Yatagai, "Holographic three-dimensional display synthesized from three-dimensional Fourier spectra of real existing objects," Opt. Lett. **28**, 2518-2520 (2003).
4. H. Hong, "Analysis of the performance of the electric-field-driven liquid crystal lens (ELC Lens) for light of various incident angles," Liq. Cryst. **39**, 1055-1061 (2012).
5. Y.-P. Huang, C.-W. Chen, and Y.-C. Huang, "Superzone Fresnel liquid crystal lens for temporal scanning auto-stereoscopic display," J. Disp. Technol. **8**, 650-655 (2012).
6. S. M. Jung, S. H. Jang, H. D. Park, and W. S. Park, "Determination of all the resistances within a pixel of a TFT-LCD by using a three-dimensional simulation," J. Korean Phys. Soc. **44**, 190-194 (2004).
7. J. W. Goodman, *Introduction to Fourier Optics*, 2nd ed. (McGraw-Hill, New York, USA, 1996), pp. 63-125.
8. D. Blinder, A. Ahar, A. Symeonidou, Y. Xing, T. Bruylants, C. Schretter, B. Pesquet-Popescu, F. Dufaux, A. Munteanu, and P. Schelkens, "Open access database for experimental validations of holographic compression engines," in *Proc. Seventh International Workshop on Quality of Multimedia Experience (QoMEX)* (Pylos-Nestoras, Greece, May 2015), pp. 1-6.